Supporting Information

Amorphous NiB as electrocatalyst from KA oil to succinic

Yulin Zhou[1,], Lei Zhu[1], Xiaohong Tao[1],*
Wenbin Jiang[2], Jun Chai[1,], Hangjia Shen[1,*]*

Content

1. Experimental Section

1.1. Preparation of carbon fiber

The carbon fiber (CF) cut into slices (~2 cm × 2 cm) and ultrasonicated in acetone, ethanol, deionized water, and HNO_3 (40 wt%) for 30 min successively. Then, the CF was followed by washing thoroughly with ethanol and water successively, dried at 60 °C for further use.

1.2. Preparation of NiB/CMK-3 and the working electrode

In a typical preparation, 20 mg of CMK-3, 1 mL of solution A (0.2 g of $NiCl_2 \cdot 6H_2O$ dissolved in 50 mL of deionized water) were dispersed in 20 mL of deionized water under ultrasonic processing for 30 min to form a uniform solution. Subsequently, 5 mL of fresh solution B (30 mg of $NaBH_4$ dissolved in 5 mL of deionized water) were added into the solution dropwise over 2 h under vigorous stirring. The mixed solution was then transferred to a round-bottom flask (50 mL) and maintained at 140 °C for 1 h in a nitrogen atmosphere. The NiB/CMK-3 NPs were then filtered from the solution, followed by drying at 60 °C in a vacuum for 24 h.

The working electrode was prepared by dispersing 8 mg of NiB/CMK-3 (or other prepared catalysts) and 0.1 mL of Nafion (5%) in 1.0 mL of ethanol for 30 min ultrasonic processing to form a uniform solution. The solution was added dropwise onto the carbon fiber (~2 cm × 2 cm) and placed under an infrared lamp to dry. The catalysts loading on the carbon fiber was calculated to be approximately 2 $mg \cdot cm^{-2}$.

1.3. Characterization

The morphology of the samples was characterized by TEM using a Tecnai G2F30S-Twin microscope equipped with a field emission gun operated at 300 kV. Energy dispersive X-ray (EDX) mapping and high angle annular dark field-scanning TEM images were analyzed using a FEI Titan G2 80-200 ChemiSTEM. Structural

images were obtained by scanning electron microscopy (SEM) using a Hitachi FE-SEM S-4700 operated at 15.0 kV. XRD was performed on a Bruker D8 X-ray diffractometer at a scan rate of $0.05°s^{-1}$. XPS analysis was performed on a Escalab250xi XPS system. Ni K-edge and Pt L3-edge XANES spectra were collected on the BL14W1 beamline at Shanghai Synchrotron Radiation Facility.[1] The samples were mounted on a high-precision five-dimension sample stage, of vertical and horizontal translations in micrometer precision, with a goniometer to tilt the sample (±3°) along the X-ray beam and another goniometer to rotate (180°) the sample in the beam. The XAFS spectra were collected in the fluorescence mode with the Si (111) double-crystal monochromator. For energy calibration, a XAFS spectrum of standard copper foil was measured in transmission mode. Data was analyzed and plotted using the Athena software. Copper was suitable as a characterization standard in XAFS experiments.

1.4. Computational Methods

Density functional theory (DFT) calculations were conducted using the Vienna *ab initio* simulation package (VASP)[2-3]. The Perdew-Burke-Ernzerhof (PBE) generalized gradient approximation was employed to describe the exchange-correlation functional[4]. Projector augmented wave (PAW) potentials[5] were employed to represent core-valence interactions. The Brillouin zone was sampled using a Γ-centered k-point grid, with spin-polarization implemented throughout all calculations. To accurately describe the localized character of nickel 3*d* orbitals, a Hubbard U correction of 5.4 eV was applied. The plane-wave basis was set to be 544 eV. The convergence criteria are 1.36×10^{-8} eV for total energy and 0.01 eV/Å for force. The vacuum region was set to be 15 Å to avoid the interactions between the adjacent layers. To accurately capture the dispersion interaction within water adsorption systems, Vander Waals correction was considered by adopting the Grimme's DFT-D3 method with zero-damping function[6].

2. Electrochemical measurements

On LSV and CV tests, the measurements of HER and ECO for cyclohexanone and cyclohexanol were conducted using a three-electrode system with a CHI 660D electrochemical workstation (CH Instruments, Inc., Shanghai). In this setup, carbon cloth (1 cm × 1 cm) covered with NiB/CMK-3 catalyst was used as the working electrode, while platinum foil electrode (2 cm × 2 cm) and Ag/AgCl electrode (in 3 M KCl solution) served as the counter and reference electrodes, respectively. The ECO of cyclohexanone and cyclohexanol experiments were similar with HER, except that the electrolyte conducted in 1 M KOH solution with 10 mM cyclohexanone or cyclohexanol**.** The potentials were converted to a RHE scale using the following Nernst equation: (E(RHE) = E(Ag/AgCl) + 0.059 pH + 0.197). All the LSV measurements were iR-compensated to account for the voltage drop between the reference and working electrodes. The scan rate for LSV was kept at 5 mV s^{-1}.

ECO of cyclohexanone experiments were performed in a two-electrode H-cell system with a Nafion-117 membrane. A 1 M KOH solution (10 mL) containing 10 mM cyclohexanone was used in the anode chamber, while 10 mL of a 1 M KOH solution were used in the cathode chamber. The carbon cloth (~2 cm × 2 cm) with NiB/CMK-3 was used as the cathode electrode, while platinum electrode (2 cm × 2 cm) was used as the anode electrode. The electrocatalytic reaction was performed at 60 °C with a 20 mA constant current provided by GPD-4303S (constant current power supply) for 2 h. ECO of cyclohexanol experiments were performed in the same condition as ECO of cyclohexanone experiments except the cyclohexanone substrate was replaced by cyclohexanol.

In order to analyze the products, 100 μL of the electrolyte solution were periodically collected from the electrolyte solution during the reaction. The final samples were pretreated and then analyzed by GC (FuLi GC9790II) and HPLC (Agilent 1260) to calculate the conversion of guaiacol and selectivity of cyclohexanol and cyclohexanone.

The concentration of cyclohexanone and cyclohexanol was detected by GC. The sample solution was extracted by ethyl acetate before inject. The area of these substances appearing in GC spectra is proportional to the concentration of these in sample solution. The GC standard curve of cyclohexanone and cyclohexanol are show on Figure S1.

Succinic acid, glutaric acid, and adipic acid are main detected product by HPLC. The sample solution is strong alkaline which was harmful to the HPLC column. Therefore, the sample solution is first diluted tenfold and neutralized by acid before inject. The area of them appearing in HPLC spectra is proportional to the concentration of them in sample solution. Standard gradient HPLC curves of succinic acid, glutaric acid, adipic acid were made and shown on Figure S2.

3. Electrochemical calculation method

The guaiacol conversion (%) and the selectivity (%) of hydrogenation products were calculated using equations (1), (2) and (3).

cyclohexanone conversion

$$Cyclohexanone\ conversion\ (\%) = \frac{mol\ of\ Cyclohexanone\ consumed}{mol\ of\ inital\ Cyclohexanone} \times 100\% \quad (1)$$

$$Cyclohexanol\ conversion\ (\%) = \frac{mol\ of\ Cyclohexanol\ consumed}{mol\ of\ inital\ Cyclohexanol} \times 100\% \quad (2)$$

$$Selectivity\ of\ Succinic\ acid(\%) = \frac{mol\ of\ Succinic\ acid\ formed}{mol\ of\ Cyclohexanone\ consumed} \times 100\% \quad (3)$$

$$Selectivity\ of\ Glutaric\ acid(\%) = \frac{mol\ of\ Glutaric\ acid\ formed}{mol\ of\ Cyclohexanone\ consumed} \times 100\% \quad (4)$$

$$Selectivity\ of\ Adipic\ acid(\%) = \frac{mol\ of\ Adipic\ acid\ formed}{mol\ of\ Cyclohexanone\ consumed} \times 100\% \quad (5)$$

The Faradaic efficiency of total diacids formation was calculated using the equation (6):

$$FE\ (\%) = \frac{mol\ of\ Succinic\ acid\ formed \times n_{SA} + mol\ of\ Glutaric\ acid\ formed \times n_{GA} + mol\ of\ Ad}{total\ charge\ passed/F} \quad (6)$$

n_{SA}: number of electrons transferred from Cyclohexanone to Succinic acid

n_{GA}: number of electrons transferred from Cyclohexanone to Glutaric acid

n_{AA}: number of electrons transferred from Cyclohexanone to Adipic acid

Where F is the Faraday constant (96485 C mol^{-1}), the potentials were converted to a RHE scale using the following Nernst equation:

$$E_{(RHE)} = E_{(Ag/AgCl)} + 0.059\ pH + 0.197$$

4. Supplementary Results

Table S1 Comparison of reaction result under varied experimental condition.

Entry	Key Parameter	SA	GA	AA	Cyclohexanone	Conv.	F.E. (SA)
		Concentration (mmol/L)					
1	At 60 °C	4.21	0.30	0.69	1.83	81.7%	55.0%
2	At 20 °C	1.73	0.07	0.38	6.23	37.7%	22.6%
3	1,4-cyclohexanedione[a]	5.76	0.08	0.23	-	93.4%	57.9%

Data were analyzed from the electrolyte after 1 h of reaction.

[a]: 1,4-Cyclohexanedione was used as the substrate instead of cyclohexanone.

Table S2 The mass fraction of Ni and B percentage of NiB/CMK-3 measured by ICP.

Catalysts	Mass fraction of Ni (%)	Mass fraction of B (%)
NiB/CMK-3	2.07	0.08

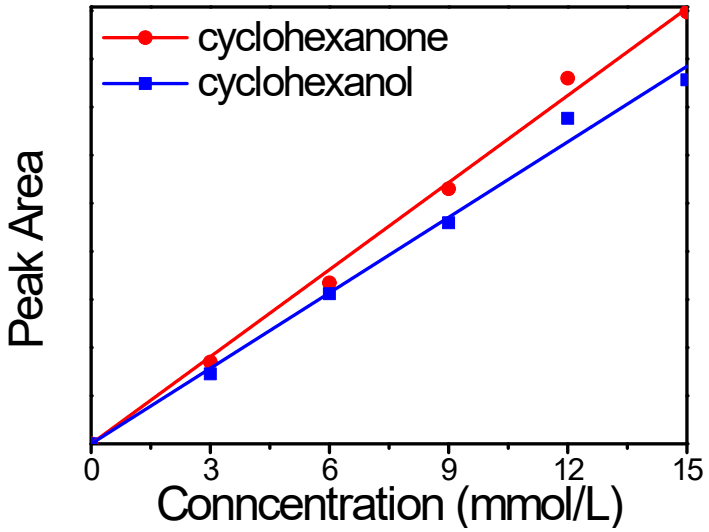

Figure S1. GC standard curve of cyclohexanol and cyclohexanone.

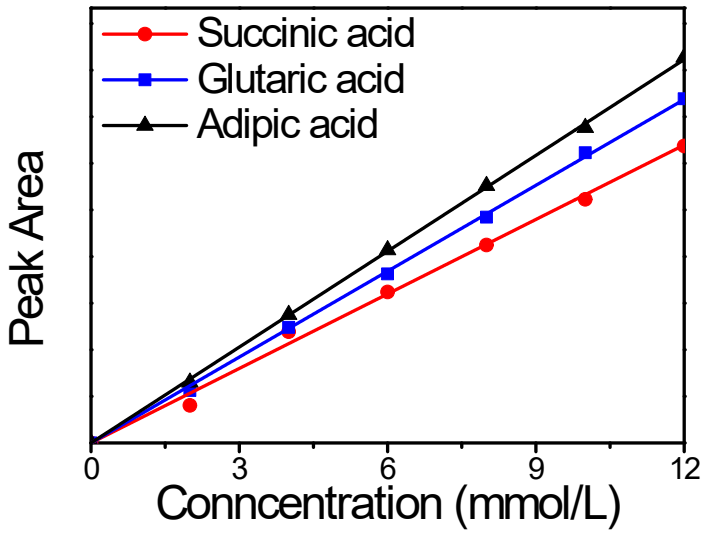

Figure S2. HPLC standard curve of succinic acid, glutaric acid, and adipic acid.

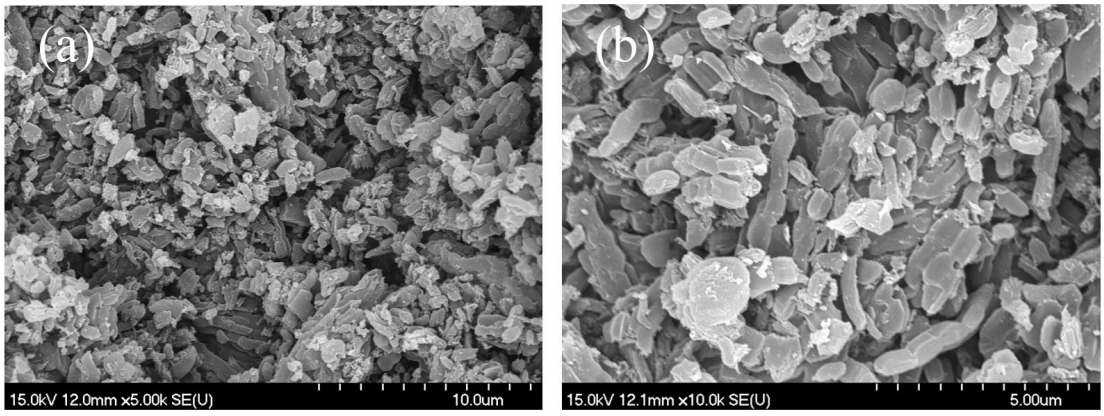

Figure S3. SEM of (a) CMK-3 and (b) NiB/CMK-3

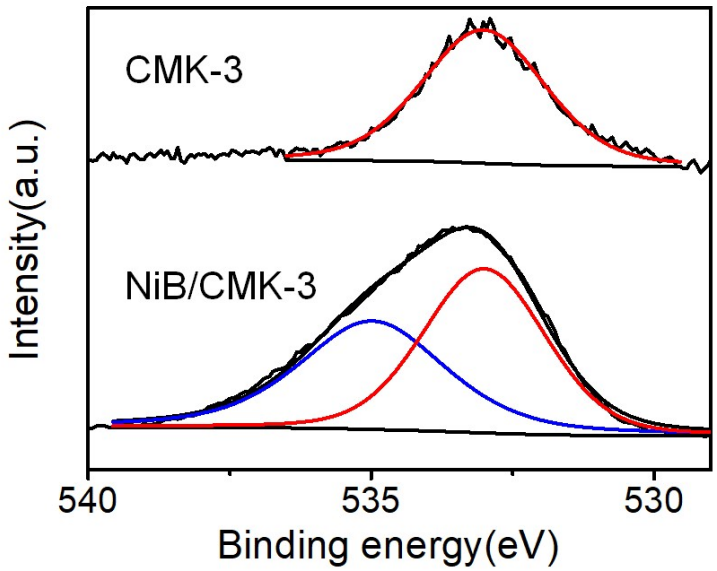

Figure S4. O 1s XPS spectra of CMK-3 and NiB/CMK-3.

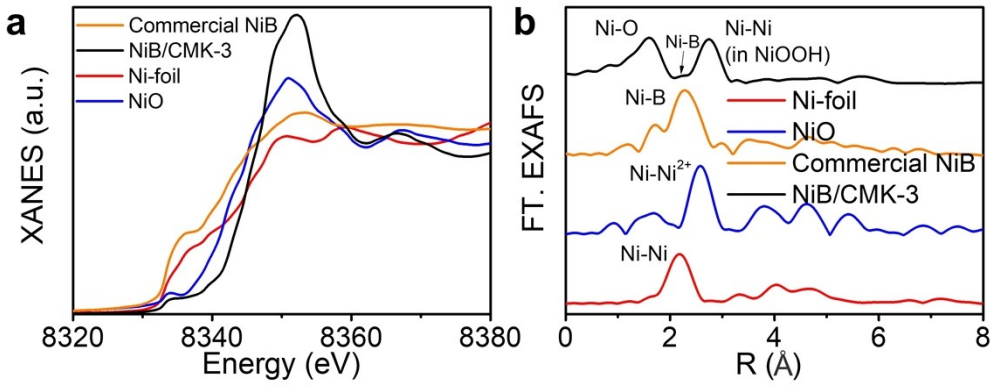

Figure S5. (a) Ni K-edge XANES spectra and (b) EXAFS spectra of Ni foil, NiB/CMK-3, Commercial NiB, and NiO.[7]

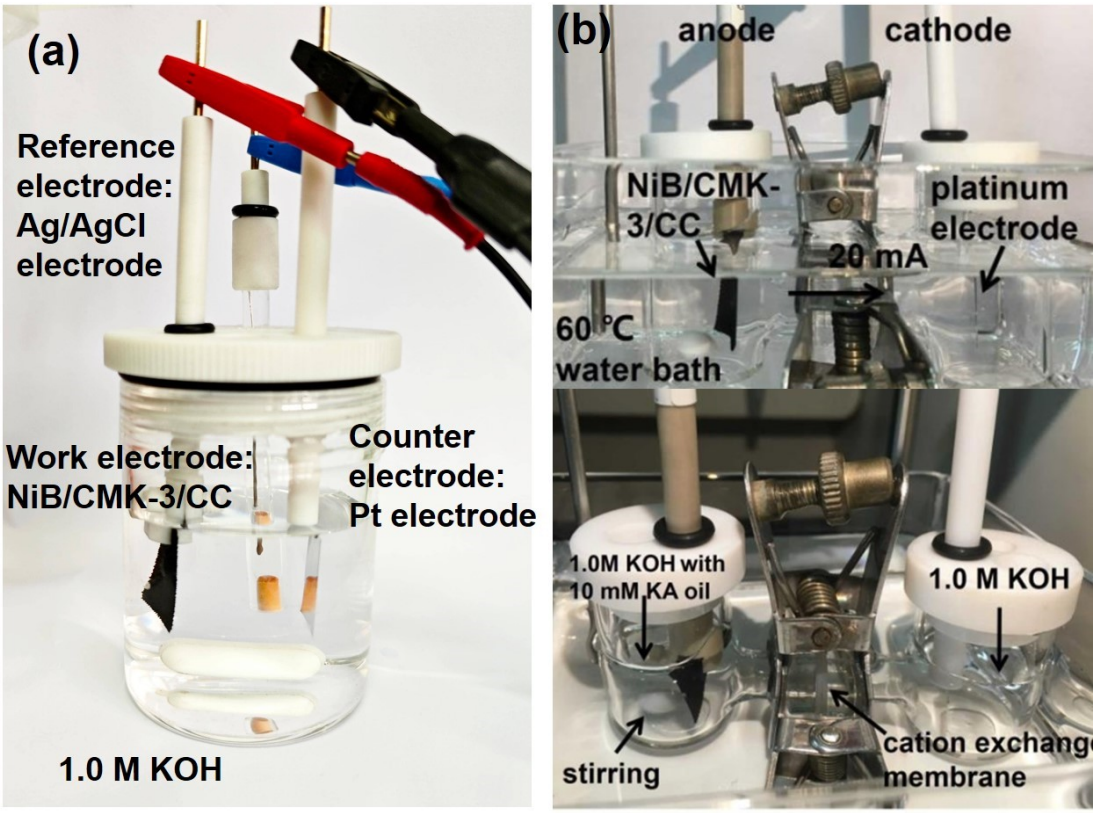

Figure S6. (a) three-electrode setup used for the LSV; (b) The H cell for ECO of KA oil.

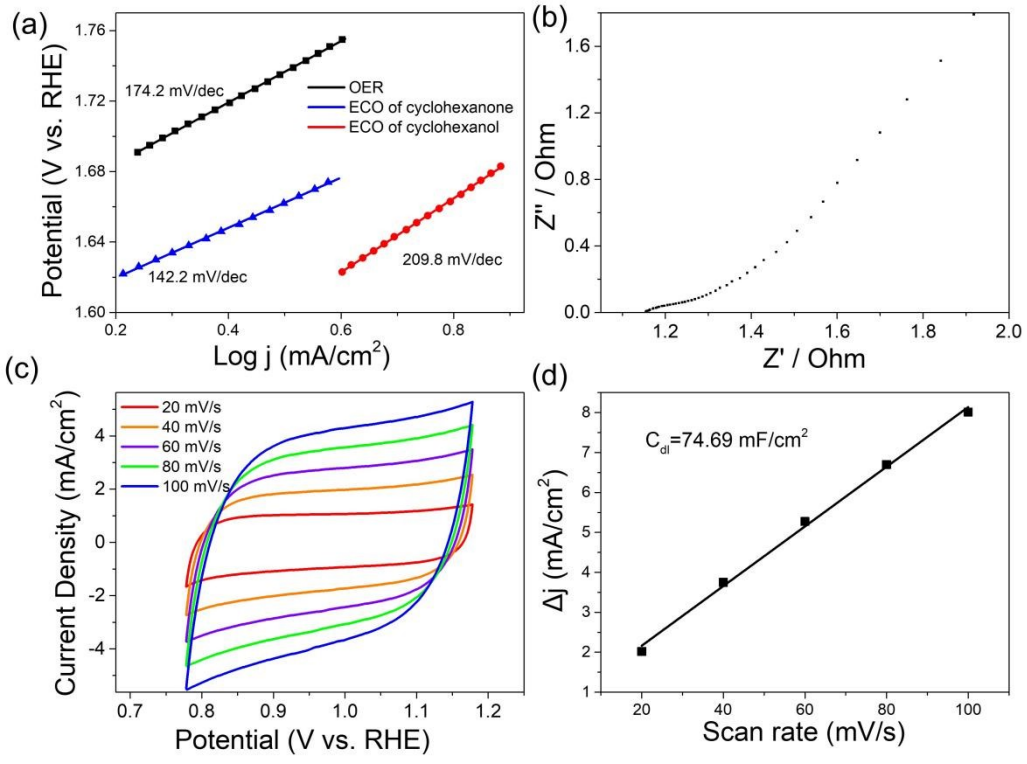

Figure S7. Electrochemical performance of NiB/CMK-3. (a) Comparison of Tafel

slopes derived from LSV for OER and ECO processes. (b) Nyquist plots. (c) Cyclic voltammograms measured at different scan rates. (d) Linear fitting of capacitive current against scan rate for double-layer capacitance calculation.

5. References

1. Yu, H. S.; Wei, X. J.; Li, J.; Gu, S. Q.; Zhang, S.; Wang, L. H.; Ma, J. Y.; Li, L. N.; Gao, Q.; Si, R.; Sun, F. F.; Wang, Y.; Song, F.; Xu, H. J.; Yu, X. H.; Zou, Y.; Wang, J. Q.; Jiang, Z.; Huang, Y. Y., The XAFS beamline of SSRF. *Nucl. Sci. Tech.* **2015,** *26* (5), 7.
2. Kresse, G.; Furthmüller, J., Efficiency of ab-initio total energy calculations for metals and semiconductors using a plane-wave basis set. *Computational Materials Science* **1996,** *6* (1), 15-50.
3. Kresse, G.; Furthmüller, J., Efficient iterative schemes for ab initio total-energy calculations using a plane-wave basis set. *Physical Review B* **1996,** *54* (16), 11169.
4. Perdew, J. P.; Burke, K.; Ernzerhof, M., Generalized gradient approximation made simple. *Physical Review Letters* **1996,** *77* (18), 3865.
5. Blöchl, P. E., Projector augmented-wave method. *Physical Review B* **1994,** *50* (24), 17953.
6. Grimme, S.; Antony, J.; Ehrlich, S.; Krieg, H., A consistent and accurate ab initio parametrization of density functional dispersion correction (DFT-D) for the 94 elements H-Pu. *The Journal of Chemical Physics* **2010,** *132* (15), 154104.
7. Zhou, Y.; Gao, Y.; Zhong, X.; Jiang, W.; Liang, Y.; Niu, P.; Li, M.; Zhuang, G.; Li, X.; Wang, J., Electrocatalytic Upgrading of Lignin‐Derived Bio‐Oil Based on Surface‐Engineered PtNiB Nanostructure. *Advanced Functional Materials* **2019,** *29* (10), 1807651.1-1807651.11.